

## Three-dimensional organization of rat hepatocyte cytoskeleton: relation to the asialoglycoprotein endocytosis pathway

P. M. Novikoff\*, M. Cammer, L. Tao, H. Oda, R. J. Stockert, A. W. Wolkoff and P. Satir

Departments of Pathology, Anatomy & Structural Biology and Medicine, Albert Einstein College of Medicine, 1300 Morris Park Avenue, Bronx, NY 10461, USA

\*Author for correspondence at Department of Pathology

### SUMMARY

Analysis by confocal microscopy has revealed features of the microtubule network of rat hepatocytes in culture, establishing the three-dimensional disposition of the microtubule-based cytoskeleton, its relation to the actin-based cytoskeleton and to ligand-containing endosomes during receptor-mediated endocytosis and the alterations in its structure and disposition by the microtubule pertubant, Taxol. By co-localization studies, we have been able to demonstrate that the microtubules have a significant role in receptor-mediated endocytosis of asialoglycoproteins in this cell. Asialoorosomuroid-containing endosomes attach to widely spaced arrays of microtubules running under the baso-lateral surface of the hepatocytes 5-15 minutes after the initiation of endocytosis and then travel along microtubule paths to become concentrated with microtubules near the centrosome and at bile canaliculi after 30-60 minutes of receptor-mediated endocytosis. Receptor-

mediated endocytosis is affected, but not abolished by Taxol, which inhibits the rate of asialoorosomuroid degradation at the same concentrations as those that disrupt microtubule and cytoplasmic dynein distribution, and that prevent the concentration of endosomes centrally. The results support suggestions that asialoorosomuroid-containing endosomes are captured by microtubules just below the actin layer at the cell periphery and these are actively transported centrally along microtubules, possibly by cytoplasmic dynein, so that the concentration of endosomes near the centrosome, and the subsequent efficient lysosomal degradation of ligand, are consequences of the confluence of microtubules in this region.

Key words: Microtubule, Receptor-mediated endocytosis, Taxol, Actin, Cell polarity, Centriole, Microtubule organizing center, Tubulin, Dynein

### INTRODUCTION

Although receptor-mediated endocytosis (RME) has been extensively studied in a variety of cells for a number of years (for reviews see Goldstein et al., 1985; Simons and Fuller, 1985; Mellman et al., 1986; van Deurs et al., 1989; Rodriguez-Boulan and Powell, 1992; Watts and Marsh, 1992; Bu and Schwartz, 1994; Satir, 1994), most studies have either not considered nor detailed the extent to which microtubules (MTs) play a role in RME. However, a limited number of studies in several different cell types, including a few in hepatocytes in culture, have postulated the involvement of MTs in RME (Wolkoff et al., 1984; Samuelson et al., 1988; Gruenberg et al., 1989; Scheel and Kreis, 1991; Goltz et al., 1992; Herskovits et al., 1993; Jin and Snider, 1994; Apodaca et al., 1994). Although it is known that hepatocytes in short-term culture form short cords and maintain hepatocyte-specific properties (Wolkoff et al., 1985; Samuelson et al., 1988), except for the distribution of actin microfilaments in hepatocytes (Phillips, 1994), there is little information available regarding the spatial distribution of the cytoskeleton in these cells. In particular, the overall distribution of MTs, and consequently their relationship to the route taken by endosomes through the cytoplasm,

have not been thoroughly addressed. This seems particularly significant in light of the hypothesis that MTs contribute to the polarity that characterizes such pathways (Goltz et al., 1992; Oda et al., 1995). The unique structural features of the hepatocyte make clear, unobvious, testable predications as to where endosomes will be found at various times during endocytosis, if their association with MTs is functional in this cell.

Confocal microscopy provides a method of obtaining a detailed overview of cytoskeleton-membrane relationships in the whole cell. In this study, using confocal images, we undertake a three-dimensional reconstruction of the MT-based cytoskeleton of the hepatocyte. We map the three-dimensional MT distribution in relation to the bile canaliculus and other cell surfaces, in contrast to the distribution of the actin-based cytoskeleton, and in relation to several cytomembrane components, including endosomes. By co-localization we demonstrate that endosomes containing asialoorosomuroid (ASOR), endocytosed by the asialoglycoprotein receptor, attach sparsely to the widely spaced array of MTs near the surface at early times after uptake and become concentrated along MTs near the centrosome and at bile canaliculi 30-60 minutes later.

The microtubule-stabilizing drug Taxol has been used as a pertubant of microtubule organization. It is known that RME

is affected, but not abolished, by microtubule disrupting agents such as colchicine or nocodazole (Wolkoff et al., 1984; Jin and Snider, 1993; DeBrabander et al., 1988). We demonstrate that Taxol inhibits the rate of ASOR degradation at the same concentrations as it disrupts MT distribution and the distribution of the motor molecule cytoplasmic dynein, in the cytoplasm. Further, the concentration of endosomes near the centrosome is slowed in parallel with the inhibition of degradation. Taken together, these studies spatially define the microtubule pathway throughout the hepatocyte cytoplasm under various conditions. They support the hypothesis that ASOR-containing endosomes are first captured by microtubules below the actin layer near the basolateral cell surface and then transported along microtubules to a central location in the cell or onward towards the bile canaliculus. The concentration of endosomes near the centrosome is a consequence of the confluence of microtubules in this region. (Portions of this work have been published in abstract form: Novikoff et al., 1992, 1993b.)

## MATERIALS AND METHODS

### Isolation and short-term culture of rat hepatocytes

Rat hepatocytes were isolated from 200-250 g male Sprague-Dawley rats after perfusion of the liver with collagenase type IV (Sigma Chemical Co., St. Louis, MO) (Samuelson et al., 1988). Cells were suspended in medium consisting of Waymouth's 752/1 (Gibco BRL, Gaithersburg, MD) containing 25 mM HEPES, pH 7.2, 5% heat-inactivated fetal bovine serum, 1.7 mM additional CaCl<sub>2</sub>, 5 µg/ml bovine insulin, 100 i.u./ml penicillin and 0.1 mg streptomycin (Wolkoff, 1984; Goltz et al., 1992). Approximately 1.5×10<sup>6</sup> cells in 3 ml of medium were placed in 60 mm Lux culture dishes and cultured in 5% CO<sub>2</sub> atmosphere at 37°C. Approximately 2 hours later, medium was changed and cells were cultured for 16-18 hours. Other cells were cultured on type III calf skin collagen-coated glass coverslips as previously described (Wolkoff et al., 1984). Cell viability was determined to be greater than 90% as judged by exclusion of trypan blue.

### Treatment of rat hepatocytes with Taxol

After 18-24 hours, some cultures of hepatocytes were incubated in medium containing 5 µM or 50 µM Taxol (added from a 1 mM stock solution in DMSO) for 1-3 hours before processing for microscopy studies. Taxol-treated cells were compared with untreated controls from the same series and with cultures where DMSO alone was added. DMSO alone had no effect on cytoskeletal distribution. Taxol was kindly provided by Dr S. Horwitz.

### Receptor-mediated endocytosis experiments: co-localization of endosomes and microtubules

RME of ASOR by hepatocytes in culture was analyzed by in situ and biochemical procedures to determine the relation of microtubules to the endocytic process. Either single-wave or continuous RME was initiated using overnight cultures. Cells grown on collagen-coated coverslips were washed 2× with 1 ml of modified serum-free medium (SFM) (135 mM NaCl, 1.2 mM MgCl<sub>2</sub>, 0.81 mM MgSO<sub>4</sub>, 27.8 mM glucose, 2.5 mM CaCl<sub>2</sub>, and 25 mM HEPES, pH 7.2) and were incubated for 60 minutes in 1 ml of SFM at 37°C. Subsequently, 10 µl of 0.1 mg/ml solution of ASOR conjugated to Texas Red, fluorescein isothiocyanate (FITC) or gold particles was added to each plate, which was then incubated for 15, 30, 45 or 60 minutes at 37°C. After incubation, plates were washed 2× with 1 ml SFM and subsequently processed and examined for localization of ASOR conjugates and immunocytochemical localization of tubulin in MTs (described below). For single-wave endocytosis of ASOR conjugates, the

procedure was as we have previously described (Wolkoff et al., 1984; Goltz et al., 1992). Briefly, cells were incubated in 1.5 ml of SFM at 37°C for 60 minutes, then shifted to 4°C and washed. Labeled ASOR was added and cells were incubated at 4°C for 60 minutes to label surface receptors. After washing away unbound ligand, cells were incubated at 37°C for 30 or 60 minutes to permit ligand internalization and processing. Degradation of [<sup>125</sup>I]ASOR was quantified from the appearance of acid-soluble radioactivity in the medium as previously described (Wolkoff et al., 1984).

### Preparation of ASOR-conjugates

ASOR was prepared from orosomuroid by acid hydrolysis (Stockert et al., 1975); the Texas Red, FITC or gold derivatives of ASOR were prepared according to the supplier's instructions (Sigma). Texas Red and FITC were purchased from Molecular Probes (Eugene, OR); colloidal gold particles were obtained from Sigma.

### Immunocytochemistry and cytochemistry

Untreated hepatocytes and Taxol-treated hepatocytes with or without induction of RME were processed on collagen-coated coverslips for immunolocalization of the various cytoskeletal elements and membrane-bounded compartments. Hepatocytes were rinsed in microtubule-stabilizing buffer (MSB: 0.2 M sucrose; 35 mM Pipes; 5 mM MgSO<sub>4</sub>, 5 mM EGTA, 0.1 M GTP, 0.1% Triton; Luftig et al., 1977; Dabora and Sheetz, 1988) for 1 minute at 37°C, after which they were treated as follows: fixation in 0.25% glutaraldehyde or a mixture of 4% paraformaldehyde/0.1% glutaraldehyde in MSB for 5 minutes at 37°C; treatment in sodium borohydrate (Sigma), 1 mg/ml physiological buffered saline [PBS] for 30 minutes and in RNase (0.1 mg/ml PBS) for 30 minutes; exposure to the following mouse monoclonal antibodies: anti-β-tubulin (1:100 dilution) (Sigma; Boehringer-Mannheim, Indianapolis, IN); anti-dynein, intermediate chain (1:200 dilution) (Sigma), overnight at 0°C. After rinsing in PBS, hepatocytes were then exposed to a fluorescence-labeled secondary antibody (goat anti-mouse IgG labeled with FITC, Texas Red, Cy 3 or Cy 5 (Molecular Probes) for all antibodies except anti-dynein, for which a labeled IgM was used). Primary and secondary antibodies were diluted in 10% goat serum, 1% bovine serum albumin and 0.1% Tween. For localization of F-actin and stress fibers, cultures similarly fixed were exposed to either FITC or rhodamine-phalloidin (Molecular Probes) for 60 minutes at room temperature. Endosomes were labeled using ASOR conjugates as described above. Co-localization of tubulin and actin was also performed with exposure to anti-tubulin and labeled second antibody as described above followed by exposure to either rhodamine or FITC-labeled phalloidin. Controls included examination of cultures for autofluorescence, after exposure to non-specific primary antisera, after exposure to anti-tubulin and IgM-labeled secondary antibody, and after exposure to anti-dynein and IgG-labeled secondary antibody. Coverslips were mounted with anti-fade mounting medium (*N*-propyl gallate, PBS, glycerin) and examined with an inverted Nikon fluorescence microscope attached to a confocal laser imaging system. All figures are illustrations of hepatocytes cultured on collagen-coated glass coverslips except Fig. 3A-C; these illustrate hepatocytes cultured on Lux plastic dishes.

### Confocal laser microscopy

Fluorescently labeled hepatocytes were examined with a Bio-Rad MRC 600 confocal fluorescent microscope (Bio-Rad Laboratories, Hercules, CA) equipped with a krypton/argon laser and a Nikon 60× numerical aperture 1.4 Planapo objective. Serial optical sections were collected in incremental steps at 0.3-1.0 µm depending on the method of volume reconstruction or rendering. No post-acquisition processing was performed (i.e. no median filtering, no edge enhancement, etc). Black level, gain and laser intensity were set to assure no background signal, when compared to secondary antibody only or to cell blank controls, and to provide as full a 256 gray scale dynamic range as possible. Excitation intensity was set to provide bright pixels

without saturation. Kalman averaging included 8 or more images for normal speed or 4 or more for slow speed. Gamma was set at 'normal' or 'low signal' (the latter only at normal speed). The pinhole aperture was closed at 3 mm or smaller depending on method of volume reconstruction or rendering and on intensity of staining. The maximum aperture we used was 3 mm, which provides an optical section of 0.7-0.8  $\mu\text{m}$  thick (Pawley, 1990). We normally used a smaller aperture closure which results in a greater  $z$  axis resolution. Tests on 0.2  $\mu\text{m}$  rhodamine-labeled beads in our system show that, practically, the intensity in the  $z$  axis appears to be the same dimensions as in the  $x$  and  $y$  axes. We refer to the sequence of optical sections in the  $xy$  plane originally taken for computer reconstructions as a 'z series'. Maximum projections were performed with the Bio-Rad MRC 600 CoMos software. Determination of MT and actin filament distribution within the space of hepatocytes was aided by volume reconstruction using VoxelView (Vital Images, Fairfield, IA) running on a Silicon Graphics workstation (Silicon Graphics, Mountain View, CA). Single voxel-wide sections and thicker volume reconstructions were made in various orientations, including that perpendicular to the original confocal orientation along the  $y$  axis (i.e. showing the  $xz$  plane). The reflectance mode of the confocal microscope was used to image gold-labeled ASOR.

## RESULTS

### Distribution of microtubules in cultured hepatocytes

Fig. 1a,b,c shows the immunolocalization of  $\beta$ -tubulin and the corresponding MT network at three different levels within the volume of several hepatocytes grown on collagen-coated coverslips. Just below the surface, a starburst pattern of microtubules is found running obliquely back from the edge toward a single focus (Fig. 1a,b). Immunofluorescence is not increased and may even diminish near the focus, because microtubules penetrate further into the cytoplasm at that point. More centrally within the cell volume (Fig. 1c), these microtubules converge into an organizing region or centrosome, which is brightly fluorescent. Single microtubules can be traced from the cell center to the periphery (Fig. 1d). An enlargement of a centrosome region depicts microtubules outlined so distinctly that, in addition to the centriole-associated MTs, MTs curving around the centriolar region and intersecting the centriolar-emanaating MTs are seen. The curving MTs appear to define the limits of the centrosome region or structures within the region (Fig. 1d).

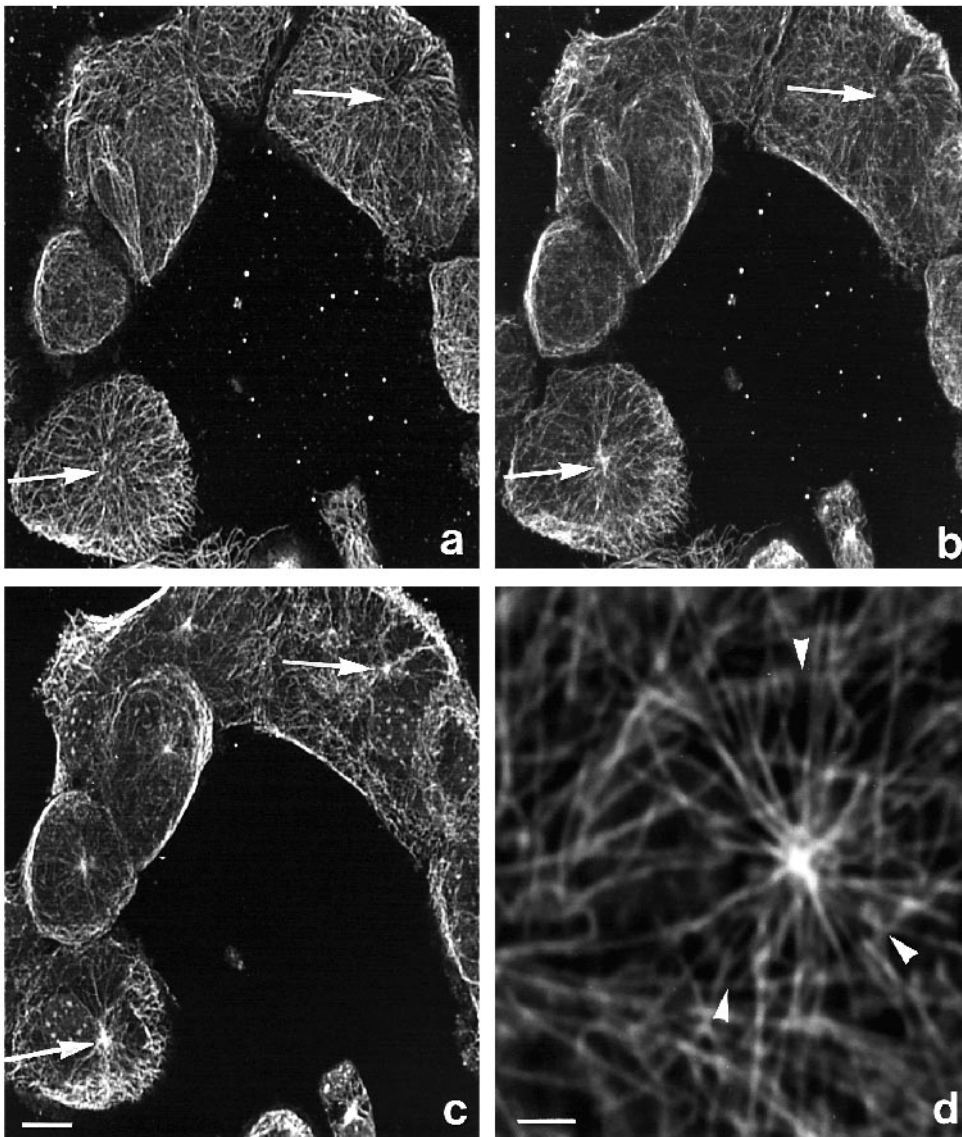


**Fig. 1.** MT distribution in cultured hepatocytes (a-d). Confocal microscopy images showing successive depths along the  $z$  axis (a) near the surface, (b) below the surface, (c) in the centrosomal and nuclear region. In a, arrows indicate confluence of tubulin-positive MT arrays directed inward in the direction of the centrosomes. In b and c, arrows indicate the centriole region beneath the area indicated in a. MTs are also seen emanating from the centriole at the level of the nucleus. (d) Detail of MTs emanating from the centriole. MTs extend linearly in a starburst pattern from the centriole. This pattern is intersected by curved MTs (arrowheads) defining the edges of the centrosphere region. Bars: (a-c) 10  $\mu\text{m}$ ; (d) 1  $\mu\text{m}$ .

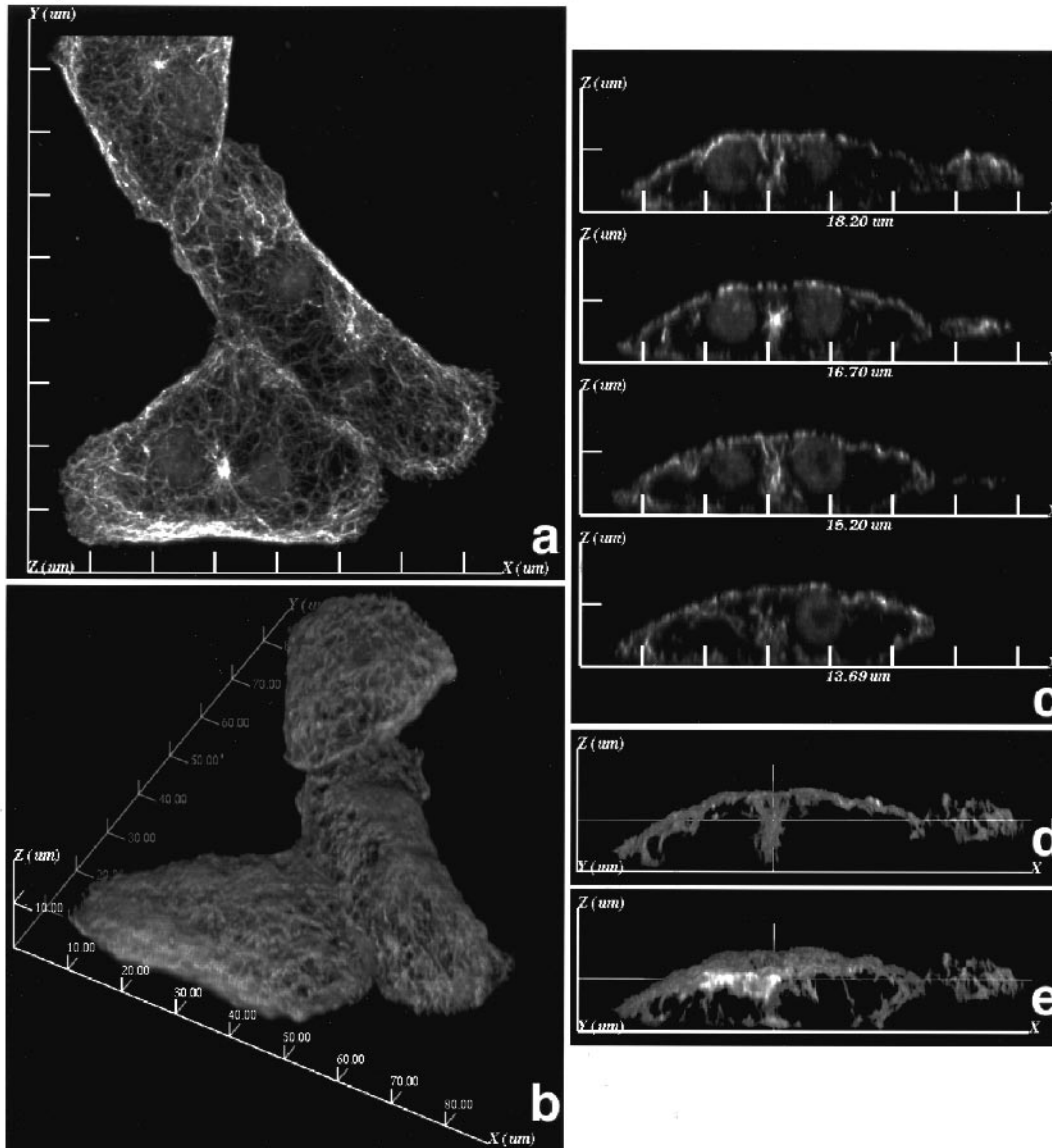


**Fig. 2.** Three-dimensional renderings of MT cytoskeleton. (a) Maximum projection of optical sections 1 through 20 of 43. The bottom half of the cells is shown. This two-dimensional projection is in the original orientation as scanned by the microscope. Calibration lines spaced at 10  $\mu\text{m}$ . (b) Volume reconstruction by VoxelView of the same cord. Volume rendering by VoxelView involves an opacity function. Brightly stained tubulin at the periphery of the cells masks the interior structure seen in a. View is from an elevation angle of  $45^\circ$  and an azimuth of  $-30^\circ$ . Numbers are in  $\mu\text{m}$ . (c) Four single voxel-wide slices sampled from the volume along the y axis and viewed in the xz plane. All slices are from the bottom cell in a. Tubulin-positive MTs are seen at the periphery and within the cytoplasm. At  $y = 16.70 \mu\text{m}$  the centriole is intersected and is visible between the two nuclei of the binucleated hepatocyte. Other slices show MTs radiating from the centriole. (d) Volume rendering of a  $7.35 \mu\text{m}$  wide slice from the region around the centriole in the bottom of a. The intensity of the voxel at the intersecting lines (near the

centriole) was used as a standard. Only contiguous voxels with intensity  $>40\%$  of this voxel are shown. The precise seed function in VoxelView was used to obtain these images. The partial volume rendering is a three-dimensional reconstruction from the single slices. The 'umbrella' appearance of the MTs is readily seen. (e) Same as d except a volume rendering of a  $12.33 \mu\text{m}$  wide slice from the region around the centriole in the bottom of a. More MT staining is seen at the periphery than in d.

An extensive analysis of the centrosome-associated microtubules has been performed by slicing the hepatocyte through  $x$ ,  $y$  and  $z$  axes for computerized tomography and volume reconstruction (Fig. 2a-e). This analysis convincingly illustrates the concentration of microtubules near the centrosome region (the 'centrosphere') and the umbrella-like manner in which a majority of the centrosome-associated microtubules flow toward the unattached surface of the cell as a compact bundle (the handle), then radiate laterally, first in the  $x,y$  direction (like umbrella ribs) under the unattached (non-collagen) surface and then in a  $y,z$  direction to line the periphery (Fig. 2c-e). A lesser number of MTs similarly extend to the attached (collagen) surface. The average height ( $z$  axis) of a hepatocyte is approximately  $35 \mu\text{m}$  but cells spread and usually are flatter. The cells shown here have heights of

approximately  $17\text{--}20 \mu\text{m}$ . Many individual microtubules running parallel to one another span the entire length of a peripheral surface. Some MTs also extend directly to each of the peripheral surfaces with high concentrations near the bile canaliculi. Voxel-view renditions (Fig. 2b) show that after overnight culture the hepatocytes lie or grow in cords, attached to each other in an arrangement reminiscent of that seen in rat liver tissue.

#### Distribution of actin filaments and polarity of hepatocytes

Using rhodamine-phalloidin, we confirmed that actin microfilaments are distributed as a thin belt around the entire periphery of hepatocytes (Fig. 3). The actin belt of nearly uniform size subtends all surfaces. In contrast to the MT localization, there

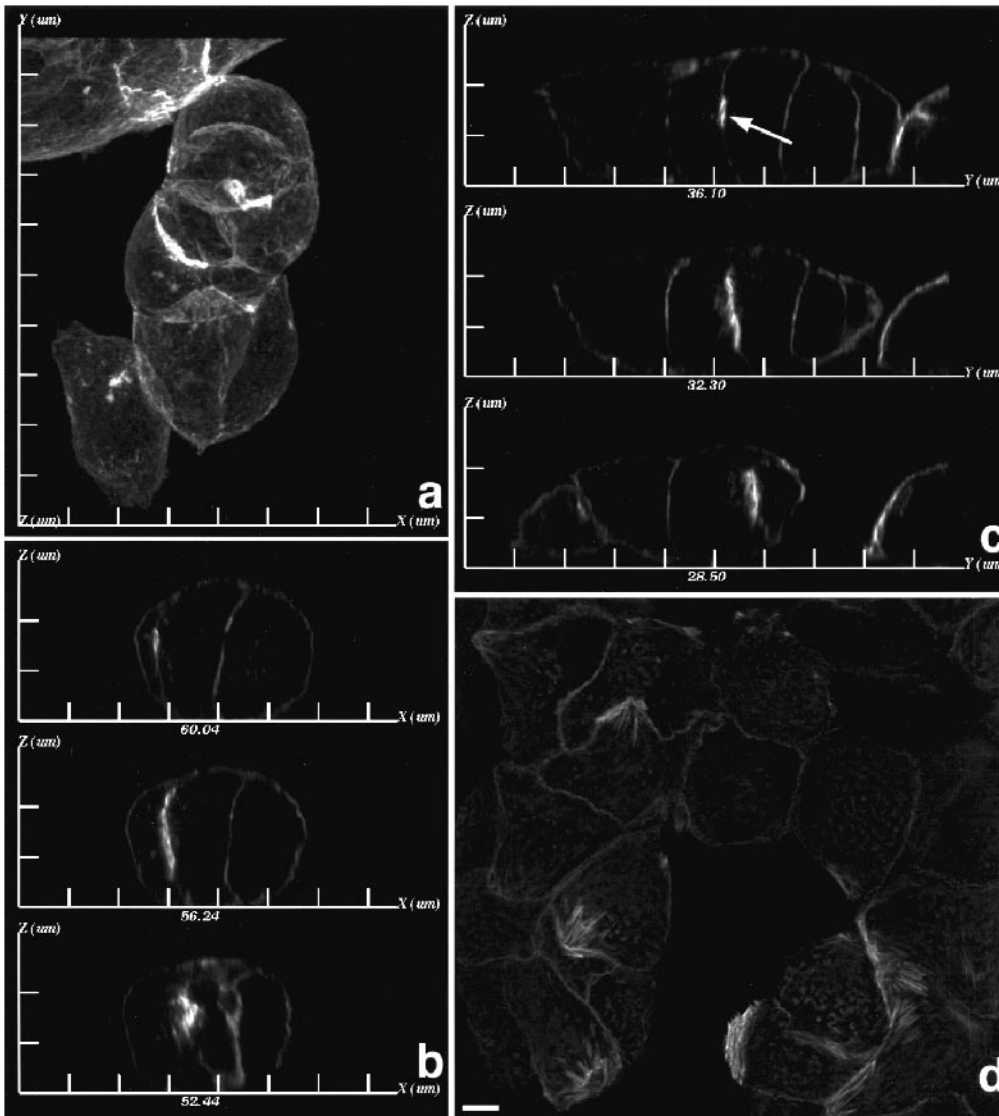


**Fig. 3.** F-actin cytoskeleton localization in a cultured hepatocyte cord. (a) Maximum projection of optical sections 1 through 73 of 73. This projection is in the original orientation as scanned by the microscope. Calibration lines spaced at 10  $\mu\text{m}$  intervals. (b and c) Three single voxel-wide slices sampled from the volume of the cells in a, along the y and x axis, respectively. F-actin, localized by rhodamine-phalloidin, is distributed around the entire hepatocyte surface with higher concentrations at the bile canaliculi, and in cytoplasmic punctate structures. Note that the bile canaliculus (arrow in c) between contiguous hepatocyte lateral surfaces, does not extend to the attached or unattached surfaces of the cord. Hepatocytes in these figures were grown on plastic dishes and appear rounder than those grown on collagen-coated glass coverslips. (d) Single optical section at the attached surface showing bundles of stress fibers stained with rhodamine-phalloidin. Hepatocytes were grown on collagen-coated coverslips. Stress fibers are organized from foci at the cell borders along collagen substratum. Actin staining is also seen in punctate structures that could represent attachment feet.

is minimal F-actin in the cytoplasm (Fig. 3b,c). In sections this F-actin is found in a scattered punctate pattern, but three-dimensional reconstruction shows that these F-actin foci are probably short, densely packed filament bundles. Foci of stress fibers and presumably attachment feet were detected at the surface of the hepatocytes exposed to collagen (Fig. 3d).

When cord-like arrangements develop in culture, bile canaliculi form between contiguous hepatocytes. In views of the cord, the bile canaliculus appears as an enclosed surface separated from the basolateral surfaces (Fig. 3b,c). High concentrations of actin filaments surround the bile canaliculi. By electron microscopy, ATPase is found to be located at the membrane domain of the bile canaliculus with actin filaments in microvilli and in the cytoplasm just beneath the enzyme lead phosphate reaction product (not illustrated).

#### Interrelations of microtubules and actin

To determine the relationships between the distribution of MTs and actin filaments, we co-localized tubulin and actin. Fig. 4 shows the distribution of MTs and actin in a section approximately through the center of a hepatocyte cord. Co-

localization confirms that the cytoplasm is filled with centrosome-associated MTs (Fig. 4a), while actin is found more sparsely in the body of the cell (Fig. 4b). The punctate distribution of small actin fibers is found between the centriole and the cell surface, especially below the bile canaliculus. Subtending the non-junctional cell membrane at both sides of the cord, bundles of actin microfilaments run with their long axis aligned with the long axis of the cord. At junctional surfaces there is particular concentration in and just under the bile canaliculi. The MTs generally are found just below and perpendicular to the actin bundles. A section of a canaliculus shows red fluorescence in and around the lumen, corresponding to actin-containing microvilli in the lumen and a delimiting actin bundle (Fig. 4c). These are ensheathed in an overlapping MT basket (yellow and green fluorescence) comprised largely of parallel plates of MTs at the opposing cell faces, such that the MTs are optically cut in cross-section when the actin microfilaments are longitudinally displayed. Although most of the MTs near the bile canaliculus run parallel to one of the edges, MTs loop perpendicularly into the plate from the cytoplasm.

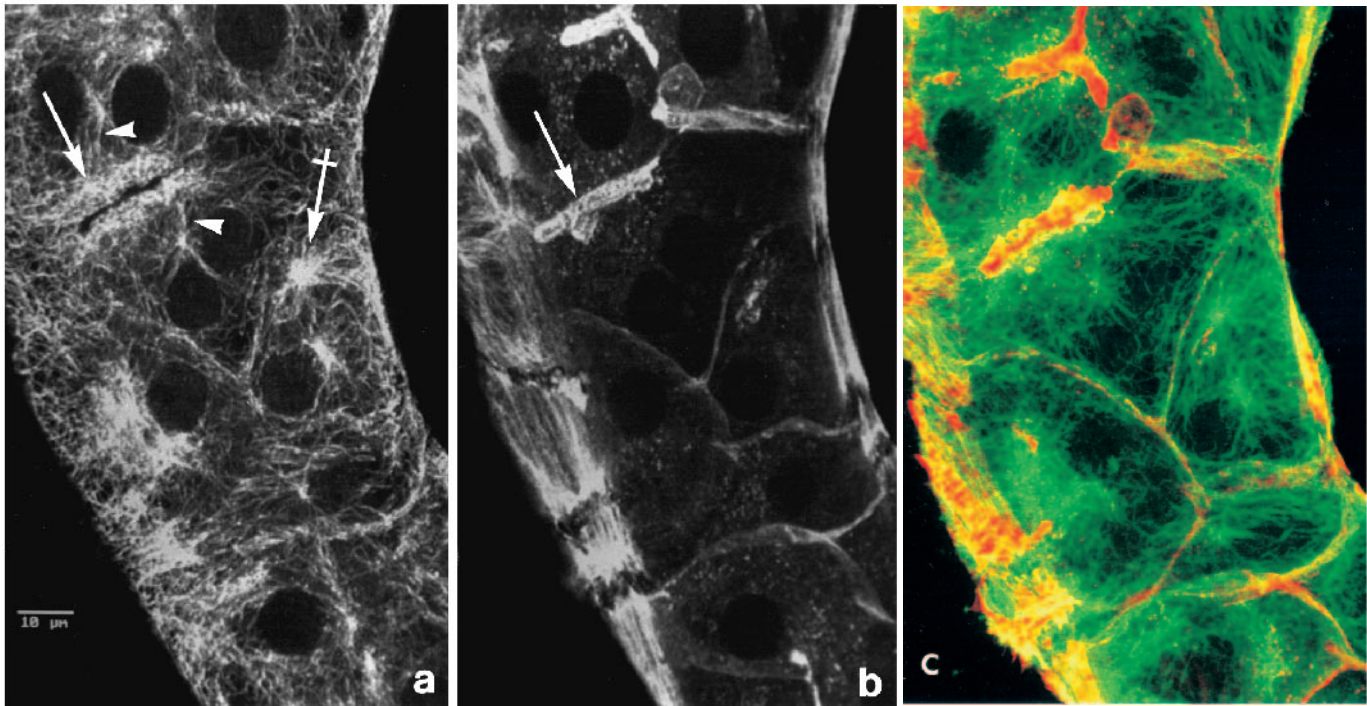


**Fig. 4.** Co-localization of MTs and actin microfilaments within a hepatocyte cord. Maximum projection of serial optical sections over about 4.5  $\mu\text{m}$  through the center of the cell. (a) Tubulin-positive MTs are distributed throughout the cytoplasm. Note the web of MTs (arrow) beneath the bile canaliculus and the concentration of MTs extending from the centriole (crossed arrow) to the surface and to the bile canaliculus (arrowheads). The distribution confirms the reconstructions in Fig. 2. Bar, 10  $\mu\text{m}$ . (b) Actin filaments. There are few filaments in the cytoplasm, but many are distributed just below and parallel to the hepatocyte surface. The distribution confirms the reconstruction shown in Fig. 3. Note the dense web of actin at the bile canaliculi (arrow) and the small actin foci in the adjacent cytoplasm. (c) Colocalization of MTs (green) and actin filaments (red); yellow color indicates overlap. MTs and actin filaments crisscross each other near the cell surface. Merged images are slightly different from those in a and b. Maximum projection of serial optical sections about 4.5  $\mu\text{m}$  through the center of the cells.

### Interactions of microtubules with ASOR-containing endosomes

RME was studied in relation to the MT cytoskeleton after addition of either gold or Texas Red-labeled ASOR to cultured hepatocytes in continuous endocytosis at 37°C. Fifteen minutes after the initiation of RME, labelled ASOR was visualized in confocal sections as a series of discrete points near the hepatocyte surfaces (Figs 5a,b, 7c). The points are found in the peripheral cytoplasm along the whole surface, but mainly appear distributed in linear arrays, which suggests capture and a spatial alignment along the peripheral MTs. By 30-60 minutes (Figs 5c-f, 6a-e), although some label is still seen as individual points associated with peripheral MTs, most of the label has moved to the centrosphere region where the points or packets fuse into larger masses that become highly concentrated in the cell interior and that appear to co-localize with the concentration of centrosphere-located MTs in this region. At this time we have also observed an accumulation of label in spherical structures (presumably lysosomes) near the bile canaliculus (Fig. 6b). We are aware that our interpretations are based on a methodology that has the resolution of confocal microscopy. However, ASOR-labeled endosomes are only found in regions where staining for tubulin is observed (i.e. no ASOR-labeled endosomes are seen in regions without tubulin staining, which appear as black areas in the cytoplasm).

### Effect of Taxol on receptor-mediated endocytosis

We measured the amount of labeled ASOR degraded (by delivery to lysosomes) at 60 minutes after initiation of single wave RME (Fig. 7a). In untreated hepatocytes, about 15% of total labeled ligand is degraded by this time. As seen in Fig. 7a, Taxol affects the rate of ligand degradation in a dose-dependent manner with significant inhibition in concentrations as low as 5  $\mu\text{M}$ . Upon addition of 50  $\mu\text{M}$  Taxol to the cultures, the amount of ligand degradation at 60 minutes is inhibited by over 50%.

In situ studies have been performed to determine the interactions of ASOR-containing endosomes and MTs during RME after low dose Taxol treatment. Continuous endocytosis of labeled ASOR was studied in the presence of 5  $\mu\text{M}$  Taxol. After Taxol treatment, labeled endosomes were only seen near or along altered MTs (see next section) peripheral to the centrosphere, even after 60 minutes of continuous endocytosis (Fig. 7b). The endosomes remained as a constellation of small points spread along the peripheral cytoplasm, presenting images resembling their disposition at much earlier times in controls (Fig. 7c). They never became fused and concentrated around the centrosphere. No labeled endosomes were visualized near the bile canaliculus.

### Effect of Taxol on microtubule distribution

Treating short-term cultured hepatocytes with Taxol for 1 hour

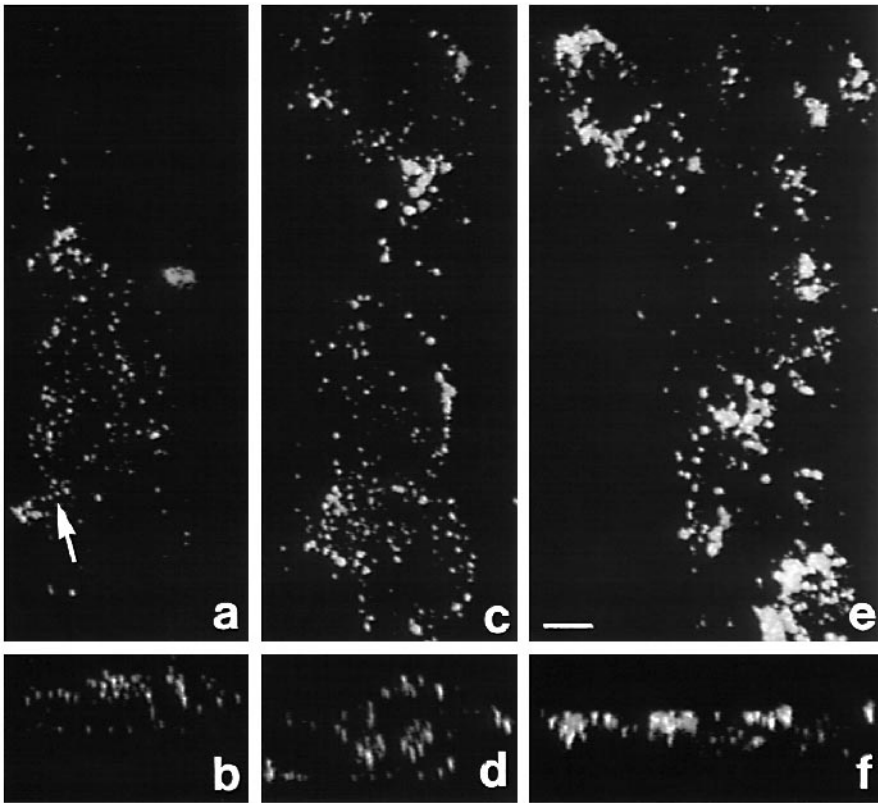


**Fig. 5.** Confocal images illustrating continuous endocytosis of Texas Red-labeled ASOR by hepatocytes in culture. (a,c,e) Images in the *xy* plane (along the *z* axis); (b,d,f) images in the *xz* plane (along the *y* axis) of uptake of ASOR after 15, 30 and 60 minutes, respectively. After 15 minutes (a,b), ASOR containing structures appear in linear arrays (arrow), with most of them at the periphery of the hepatocyte. At 30 minutes (c,d), many of the ASOR-positive structures have entered the cytoplasm and are near the cell center. At 60 minutes (e,f.), most of the ASOR-positive structures are concentrated near the cell center; compare with Fig. 6d and e. Bar, 10  $\mu$ m.

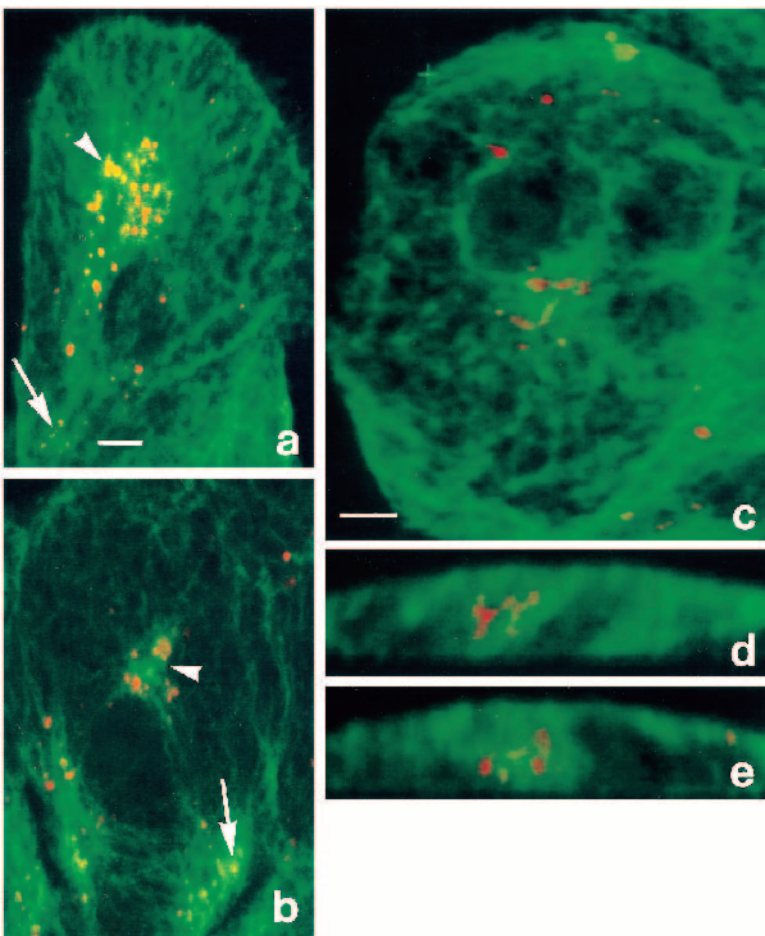


**Fig. 6.** Colocalization of Texas Red-labeled ASOR and MTs after continuous wave endocytosis for 60 minutes. In a, most of the ASOR containing structures are associated with the centrosomal MTs (green), with some seen in linear arrays over peripheral MTs (arrow). Orange and yellow images indicate overlap. ASOR-positive structures (arrowhead) follow the MTs, suggesting their distribution along the ribs of the MT umbrella (see Fig. 2c and d). In b, ASOR-positive structures are associated with the MT web near the bile canaliculus (arrow) as well as with the centrosome (arrowhead). Note the absence of ASOR-positive structures in the black regions of the cytoplasm. Analysis of the same hepatocyte in the *xy* plane (along the *z* axis) (c) and in the *xz* plane (along the *y* axis) (d,e) shows ASOR-positive structures within the centrosphere region of the hepatocyte. Bar, 10  $\mu$ m.

caused dramatic changes in the profiles and distribution of the MTs. After treatment with 5  $\mu\text{M}$  Taxol, MTs at the cell surfaces became less linear and were seen as short curved segments that appear to be more flaccid than the long straight tubules at the surfaces of untreated hepatocytes. Adjacent MT segments were closely spaced, so that a dense meshwork was formed. *z* series analysis shows that the MTs within Taxol-treated hepatocytes have altered profiles at all cell surfaces (Fig. 8a). Centrosome-associated MTs were almost totally absent in some of these hepatocytes, whereas others showed reduced numbers. For the most part, MTs are considerably less concentrated in the interior cytoplasm of Taxol-treated hepatocytes and were more concentrated at the cell periphery (Fig. 8b). This is clearly demonstrated in the series of images examined along the *y* axis (Fig. 8c,d). We also examined hepatocytes after a 3 hour exposure to 5  $\mu\text{M}$  Taxol and found that the profiles and the distribution of microtubules were essentially the same as those after 1 hour of treatment.

After treatment with 50  $\mu\text{M}$  Taxol for 1 hour, individual microtubules are no longer seen in the cells. Instead, bright patches of fluorescence probably corresponding to short bundles of altered microtubules, commonly observed in Taxol (DeBrabander et al., 1986), are formed in perinuclear regions and elsewhere in the cytoplasm (Fig. 9a).

#### Effect of Taxol on distribution of cytoplasmic dynein

We have corroborated our published findings (Oda et al., 1995) that cytoplasmic dynein localizes linearly along MTs in untreated hepatocytes under our conditions of permeabiliza-

tion. Fig. 9b shows the localization of cytoplasmic dynein in Taxol-treated hepatocytes. After treatment with 50  $\mu\text{M}$  Taxol, cytoplasmic dynein appears as patches in the cytoplasm, corresponding to the changed disposition of tubulin (Fig. 9a).

#### Effect of taxol on actin distribution

When hepatocytes are treated with 5  $\mu\text{M}$  Taxol for 1 hour, actin distribution in general remains unaltered. Actin still surrounds the cell periphery with concentration around bile canaliculi. However, bile canaliculi become dilated and prominent filopodia containing actin are found at exposed cell surfaces along the edges of the cord (Fig. 9c).

## DISCUSSION

Confocal microscopy has provided a greater understanding of the three-dimensional arrangement of the cytoskeleton in cultured hepatocytes than has previously been obtainable with conventional fluorescence and electron microscopy. With this technique in this study, the distribution of the microtubule and actin networks within the hepatocyte volume have been examined and the structural relation of the MT network to the pathway of RME has been explored. The hepatocyte represents an epithelial cell that, after isolation and plating for a short-term in culture, establishes unique apical-basolateral polarities such that pathways of vesicular trafficking in these cells are expected to be somewhat different from those in other epithelial cells. In particular, MTs in cultured primary rat hepatocytes focus at and originate presumably from a centrosome region close to the nucleus, in contrast to the MT organization in certain other cultured epithelial cells, including MDCK cells, which are widely used to study cell polarity, vesicular transport and membrane sorting signals (Lisanti et al., 1989; Sargiacomo et al., 1989; Bacallao et al., 1989; Wandingu-Ness et al., 1990), where the majority of MTs originate near the apical surface in the vicinity of the basal body of a primary cilium (Wheatley et al., 1994).

Within the centrosome region of the hepatocyte, MT organization appears more complex than previously understood. Not

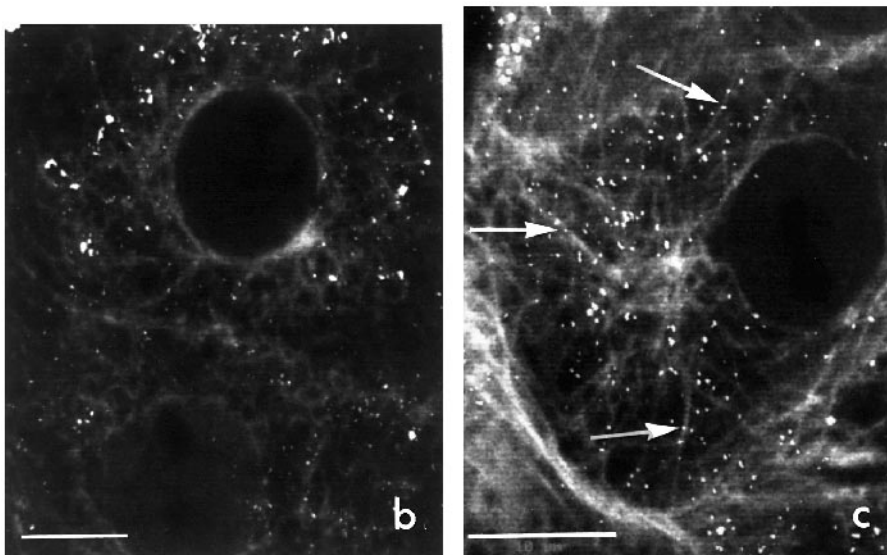
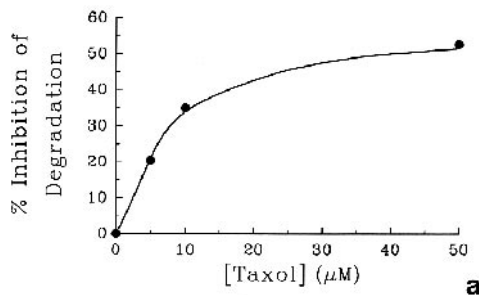


**Fig. 7.** Effect of Taxol on ASOR endocytosis. (a) Inhibition of ASOR degradation by various concentrations of Taxol. The amount of total labeled ASOR degraded after 60 minutes single wave endocytosis in control cells was compared to the amount degraded in the presence of Taxol to calculate the percentage inhibition of degradation. (b) Colocalization of Texas Red-labeled ASOR and MTs after 60 minutes continuous endocytosis in the presence of 5  $\mu\text{M}$  Taxol. (c) Co-localization of gold-labeled ASOR and MTs (arrow), after 15 minutes of continuous endocytosis in the absence of Taxol. The localization is similar in both cases: ASOR-positive structures, many in linear arrays, are seen in close association with MTs, dispersed over the cell periphery. Endosomes are essentially absent from the centrosphere region. Bars, 10  $\mu\text{m}$ .

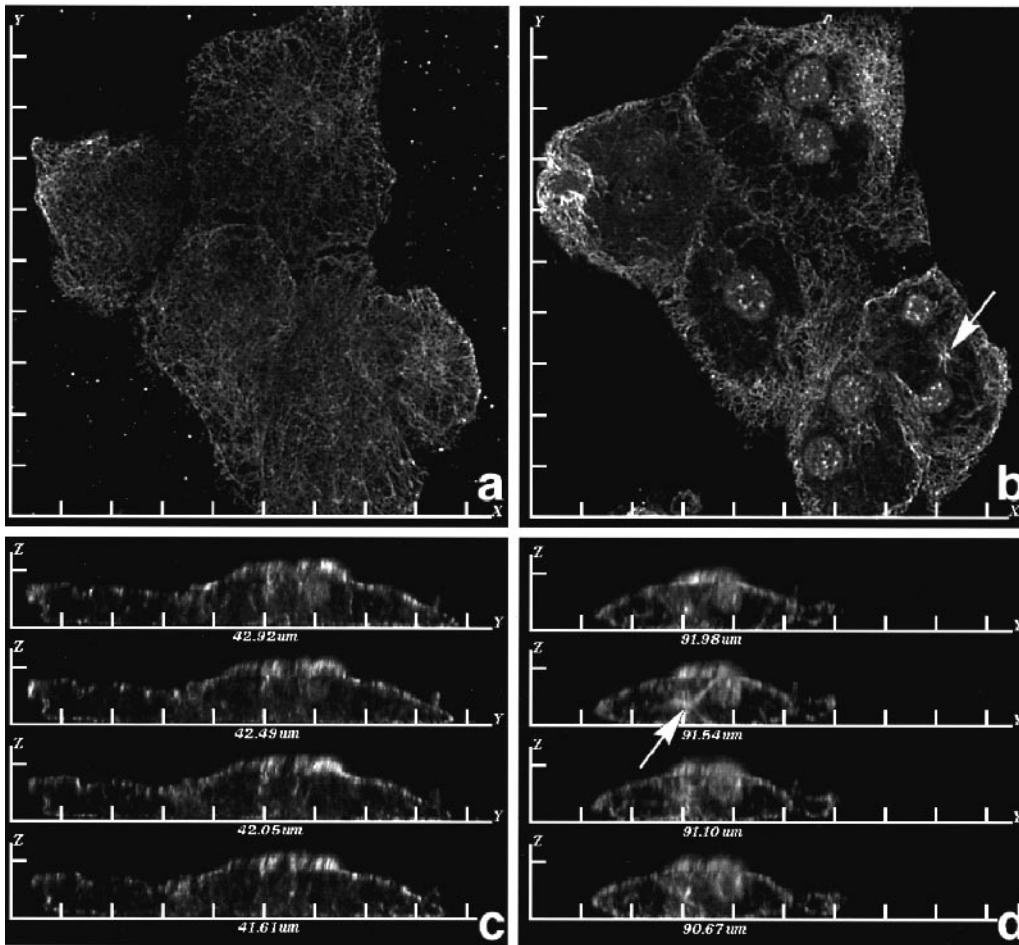


**Fig. 8.** Effect of 5  $\mu\text{M}$  Taxol on MTs. (a and b) Images in the  $xy$  plane (along the  $z$  axis) of MTs at the periphery and nuclear regions of the hepatocytes, respectively. At the peripheral surfaces, MT profiles change from linear to sinuous. Few MTs remain near the centrosome (arrows). (c and d) Images in the  $xz$  plane (along the  $y$  axis) from two different regions of the same hepatocytes. Calibration lines spaced at 10  $\mu\text{m}$ .

only do microtubules radiate out to the cell periphery, but a subset of MTs curves around the radiating MTs to outline a 'centrosphere'. This region in hepatocytes is where the Golgi apparatus (Golgi, 1898) and *trans*-Golgi network (Griffiths and Simons, 1986) (formerly termed GERL; Novikoff and Novikoff, 1977) are located. The relation of the curving centrosomal MTs to the positioning and functional cytoskeletal attachments of these membrane-bound organelles is under study. At the cell periphery, the MT array mainly consists of parallel struts, like the ribs of an umbrella. The umbrella is particularly obvious at the unattached or free surfaces of the cultured cells, but is also present at the attached surface. Both attached and free surfaces of these hepatocytes represent basolateral surfaces that probably correspond to edges of the hepatocyte cords near the space of Disse *in vivo*.

The true apical surfaces are the bile canalicular surfaces. As noted previously (Phillips, 1994), the bile canalculus of hepatocytes contains microvilli with actin core bundles and is surrounded by a well-defined actin belt, corresponding to the terminal web region of most other epithelial cells. As presented in this study, actin-phalloidin distributions to the bile canalculi (some of which show essentially similar branching patterns to those of hepatocytes *in situ*), together with ATPase colocalization (not illustrated) and previous ultrastructural observations (Samuelson et al., 1988) establish apical-basolateral polarities of these cultured rat hepatocytes. We have also localized tubulin and actin in hepatocytes *in situ* in non-frozen

liver sections prepared with a Vibratome and found similar profiles and distributions of the cytoskeletal networks (unpublished data).

Although most of the actin filaments are evident at the cell periphery, some short actin fibers are distributed within the cytoplasm, with concentrations near MTs between the centrosome and the bile canalculus. The significance of these structures is not known.

The umbrella of MTs helps define the pathway of RME from the basolateral surface to the lysosomes in the hepatocyte. Using the ligand ASOR that is readily labeled for confocal microscopy, we demonstrate that after a few minutes of continuous endocytosis, ASOR is taken up in small endosomes that can be seen linearly arranged along the surface microtubules. Later, label is found in larger masses that are concentrated at the centrosphere and near the bile canalculus. This is consistent with the work of Wolkoff et al. (1984), Goltz et al. (1992) and others, on hepatocytes, as well as studies on endosome movement in a variety of tissue culture cells (Herskovits et al., 1993; Scheel and Kreis, 1991; Jin and Snider, 1993; Bomsel et al., 1990; Gruenberg et al., 1989).

After penetrating the actin-rich membrane skeleton, prior to sorting of ligand and receptor, endosomes presumably attach to MTs and begin to move along them. In the cultured hepatocytes this motion is towards the centrosome so that it probably requires a (-)end-directed MT motor such as cytoplasmic dynein. The linear alignment of small labeled vesicles

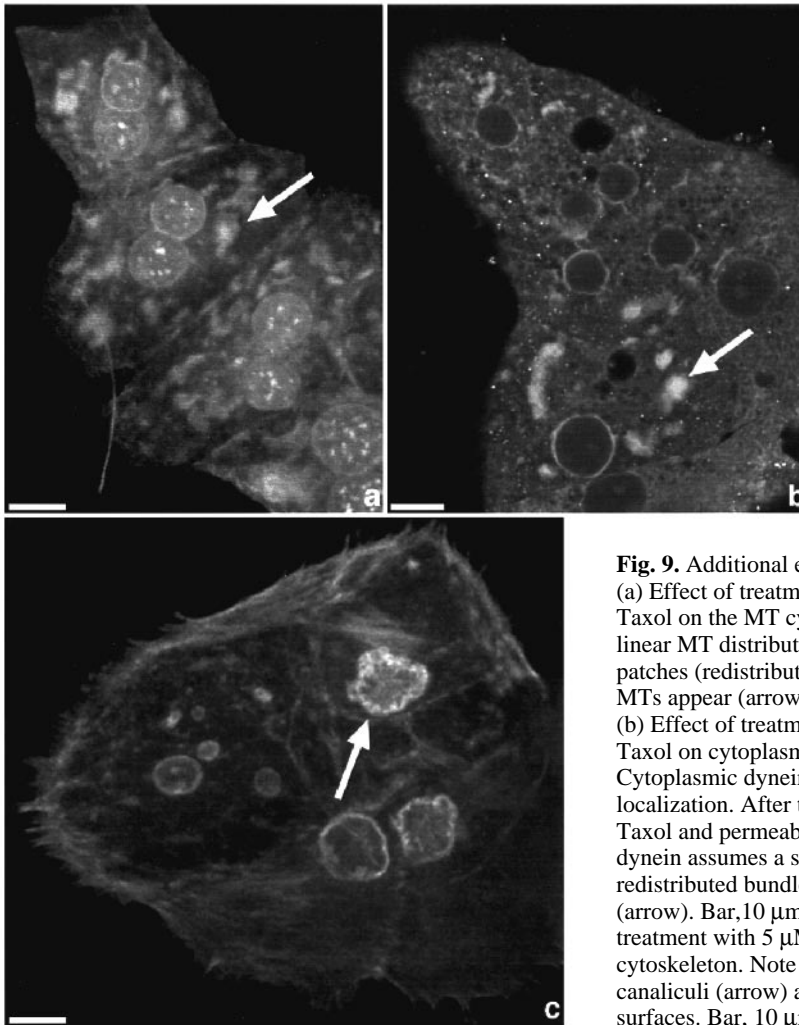


**Fig. 9.** Additional effects of Taxol. (a) Effect of treatment with 50  $\mu$ M Taxol on the MT cytoskeleton. Normal linear MT distribution is lost and thick patches (redistributed bundles) of short MTs appear (arrow). Bar, 10  $\mu$ m. (b) Effect of treatment with 50  $\mu$ M Taxol on cytoplasmic dynein. Cytoplasmic dynein parallels MT localization. After treatment with 50  $\mu$ M Taxol and permeabilization, cytoplasmic dynein assumes a similar pattern as the redistributed bundles of short MTs (arrow). Bar, 10  $\mu$ m. (c) Effect of treatment with 5  $\mu$ M Taxol on actin cytoskeleton. Note dilatation of the bile canaliculi (arrow) and filopodia at cell surfaces. Bar, 10  $\mu$ m.

that we see in the  $xy$  plane at early times after ASOR endocytosis could be a reflection of successive endosomes attached to and moving along one or a few parallel MTs below the cell surface. At later times, endosomes following such a MT pathway would be expected to move into the cell and reach the centrosphere. Consistent with this interpretation, we have recently reported that cytoplasmic dynein is associated with ligand-containing endosomes almost immediately after the initiation of endocytosis (Oda et al., 1995). We confirm the localization of cytoplasmic dynein, as well as endosomes, along the peripheral MT array (data not shown).

The dependence of RME on the intact MT cytoskeleton is illustrated by the use of perturbants such as Taxol, colchicine or nocodazole (Wolkoff et al., 1984; Goltz et al., 1992; Scheel and Kreis, 1991). Taxol, an anti-tumor drug, is thought to be cytotoxic by stabilizing polymerized MTs into bundles accompanied by redistribution of the bundles within the cytoplasm (Schiff and Horwitz, 1980; DeBrabander et al., 1986; Novikoff et al., 1993a). However, single MTs grown from tubulin and then treated with Taxol have been shown to be less linear, more flexible and wavy in appearance, rather than linear and rigid (Dye et al., 1993). When hepatocytes in culture are treated with 5  $\mu$ M Taxol, their surface MTs appear to have similarly altered flexibility, while centrosomal MTs for the most part disappear.

The effect would tend to prevent penetration of endosomes from the surface downward toward the centrosome region at even low concentrations of Taxol. Our images support this conclusion. At higher concentrations of Taxol, redistributed MT bundles are seen. Cytoplasmic dynein assumes a similar distribution to MTs in 50  $\mu$ M Taxol. These effects should lead to a more profound disruption of endocytosis.

Taxol affects endocytosis by reducing the rate of ligand degradation in a dose-dependent fashion, but, short of killing the cells, RME is not completely blocked, even when the MT cytoskeleton is dramatically altered. This is consistent with previous findings using colchicine or nocodazole (Wolkoff, 1984), which argue for an alternative default pathway of RME that is not dependent on the MT-based cytoskeleton. Although little understood, this second pathway might be of considerable importance.

Taxol also affects the actin cytoskeleton in these cells in rather interesting ways. Most significantly, the bile canaliculus becomes dilated, suggesting that the contractile tension that the actin belt maintains around the canaliculus is lessened or lost. This could be a consequence of the disappearance of the underlying microtubule plate or of other cytoplasmic conditions that accompany this disappearance. In humans and rats, Taxol is metabolized mainly by cytochrome P450 isozymes of hepato-

cyte endoplasmic reticulum and subsequently secreted into the bile via the bile canaliculi (Cresteil et al., 1994; Monsarrat et al., 1990). In the livers of rats administered Taxol, the bile canaliculus shows increased branching and dilatation (unpublished observations). The second effect is the formation of filopodia at the cell surfaces, which are smooth in controls. This too argues that the actin belt responds to the depolymerization of the underlying microtubules in an unusual and perhaps unexpected way. This mapping of the hepatocyte cytoskeletal elements with each other suggests that such interactions between actin and microtubule-based elements may regulate surface configurations and cellular responses in hepatocytes in situ to influence the patency and propulsive activity of the bile canaliculus and the speed and efficacy of vesicle processing in the cell.

In summary, we have determined the organization of a major portion of the cytoskeleton system in cultured rat hepatocytes, underscoring spatial and possible functional relations between the microtubule and actin-based systems. We have determined the spatial pathway for efficient endosomal transport in these cells. These studies now allow us to consider cytoskeletal-based cell processes that occur in hepatocytes in normal liver. Our information also has important implications for bile canalicular function. In further work, it would be interesting to explore whether Taxol metabolism is affected in parallel to its effects on the microtubule and actin cytoskeletons. This might have implications for understanding the mechanisms by which Taxol is metabolized by the liver and for its use as an agent in cancer chemotherapy.

This work was supported by NIH grants CA06576, DK41918 and DK41296. Imaging was performed at the Image Analysis Facility.

## REFERENCES

- Apodaca, G., Katz, L. A. and Mostov, K. E. (1994). Receptor-mediated transcytosis of IgA in MDCK cells via apical recycling endosomes. *J. Cell Biol.* **125**, 67-86.
- Bu, G. and Schwartz, A. L. (1994). Receptor-mediated endocytosis. In *The Liver: Biology and Pathology*, 3rd edn (ed. I. M. Arias, J. L. Boyer, N. Fausto, W. B. Jakoby, D. A. Schachter and D. A. Shafritz), pp. 259-274. Raven Press, New York.
- Bacallao, R., Anthony, C., Dotti, C., Karenti, E., Stelzer, E. H. K. and Simons, K. (1989). The subcellular organization of Madin-Darby Canine kidney cells during formation of a polarized epithelium. *J. Cell Biol.* **109**, 2817-2832.
- Bomsel, M., Parton, R., Kuznetsov, S. A., Schroer, T. A. and Gruenberg J. (1990). Microtubule- and motor-dependent fusion *in vitro* between apical and basolateral endocytic vesicles from MDCK cells. *Cell* **62**, 719-731.
- Cresteil, T., Monsarrat, B., Alvinene, P., Tielayer, J. M., Vieira, I. and Wright, M. (1994). Taxol metabolism by human liver microsomes: Identification of cytochrome P450 isozymes involved in its biotransformation. *Cancer Res.* **54**, 381-392.
- Dabora, S. L. and Sheetz, M. P. (1988). Cultured cell extracts support organelle movement on microtubules *in vivo*. *Cell Motil. Cytoskel.* **10**, 482-495.
- DeBrabander, M., Gevens, G., Nuydens, R., Wellebrods, R., Aerts, F. and De Mey, J. with the participation of McIntosh, J. R. (1986). Microtubule dynamics during the cell cycle: The effects of Taxol and Nocodazole on the microtubule system of HK<sub>2</sub> cells at different stages of the mitotic cycle. *Int. Rev. Cytol.* **101**, 215-274.
- DeBrabander, M., Nuydens, R., Geerts, H. and Hopkins, C. R. (1988). Dynamic behavior of the transferrin receptor followed in living epidermoid carcinoma (A431) cells with nanovid microscopy. *Cell Motil. Cytoskel.* **9**, 30-47.
- Dye, R. B., Fink, S. P. and William, R. C. (1993). Taxol-induced flexibility of microtubules and its reversal by MAP-2 and Tau. *J. Biol. Chem.* **268**, 6847-6850.
- Goldman, I., Jones, A. L., Hradek, G. T. and Huling, S. (1983). Hepatocyte handling of immunoglobulin A in the rat: the role of microtubules. *Gastroenterology* **85**, 130-140.
- Goldstein, J. L., Brown, M. S., Anderson, R. G. W., Russel, D. W. and Schneider, W. J. (1985). Receptor-mediated endocytosis: concepts emerging from the LDL receptor. *Annu. Rev. Cell Biol.* **1**, 1-39.
- Golgi, C. (1898). Sur la structure des cellules nerveuses des ganglions spinaux. *Arch. Ital. Biol.* **30**, 60-71.
- Goltz, J. S., Wolkoff, A. W., Novikoff, P. M., Stockert, R. J. and Satir, P. (1992). A role for microtubules in sorting endocytic vesicles in rat hepatocytes. *Proc. Nat. Acad. Sci. USA* **89**, 7026-7030.
- Griffiths, G. and Simmons, K. (1986). The trans Golgi network: sorting at the exit site of the Golgi complex. *Science* **234**, 438-443.
- Gruenberg, J., Griffiths, G. and Howell, K. E. (1989). Characterization of the early endosome and putative endocytic carrier vesicles *in vivo* and with an assay of vesicle fusion *in vitro*. *J. Cell Biol.* **108**, 1301-1316.
- Herskovits, J. S., Burgess, C. C., Obar, R. A. and Vallee, R. B. (1993). Effects of mutant rat dynein on endocytosis. *J. Cell Biol.* **122**, 565-578.
- Jin, M. and Snider, M. D. (1993). Role of microtubules in transferrin receptor transport from the cell surface to endosomes and the Golgi complex. *J. Biol. Chem.* **268**, 18390-18397.
- Lisanti, M., Le Bivic, A., Sargiacomo, M. and Rodriguez-Boulant, E. (1989). Steady-state distribution and biogenesis of endogenous Maden-Darben canine kidney glycoproteins: evidence for intracellular sorting and polarized cell surface delivery. *J. Cell Biol.* **109**, 2117-2127.
- Luftig, R. B., McMillan, P. N., Weatherbee, J. A. and Wehling, R. R. (1977). Increased visualization of microtubules by an improved fixation procedure. *J. Histochem. Cytochem.* **25**, 178-187.
- Mellman, I., Fuchs, R. and Helenius, A. (1986). Acidification of the endocytic and endocytic pathways. *Annu. Rev. Biochem.* **55**, 663-700.
- Monsarrat, B., Mariel, I., Cros, S., Gares, M., Guénard, D., Guéritte-Voegelein, F. and Wright, M. (1990). Taxol metabolism: isolation and identification of three major metabolites of Taxol in rat bile. *Drug Met. Disp.* **18**, 895-901.
- Novikoff, A. B. and Novikoff, P. M. (1977). Cytochemical contributions to differentiating GERL from the Golgi apparatus. *Histochem. J.* **9**, 525-551.
- Novikoff, P. M., Cammer, M., Wolkoff, A. W. and Satir, P. (1992). Microtubule actin filament and ER distribution in untreated and taxol-treated cultured rat hepatocytes: analysis by confocal laser microscopy. *Mol. Biol. Cell* **3**, 48a.
- Novikoff, P. M., Cammer, M., Campbell, C. and Wolkoff, A. W. (1993a). Microtubule distribution in untreated and Taxol-treated FAO hepatoma cells during interphase and mitosis: analysis by confocal microscopy. *Cancer Res.: Proc.* **34**, 289.
- Novikoff, P. M., Oikawa, I., Yam, A., Cammer, M., Stockert, R. J., Satir, P. and Wolkoff, A. W. (1993b). The rat hepatocyte cytoskeleton: Functional organization in culture and in control and regenerating livers. *Hepatology* **18**, 153a.
- Oda, H., Stockert, R. J., Collins, C., Wang, H., Novikoff, P. M., Satir, P. and Wolkoff, A. W. (1995). Interaction of the microtubule cytoskeleton with endocytic vesicles and cytoplasmic dynein in cultured rat hepatocytes. *J. Biol. Chem.* **270**, 15242-15249.
- Pawley, J. (1990). Fundamental limits in confocal microscopy. In *Handbook of Biological Confocal Microscopy* (ed. J. B. Pawley), pp. 232. Plenum Press, New York.
- Phillips, M. J. (1994). Biology and pathobiology of actin in the liver. In *The Liver: Biology and Pathobiology*, 3rd edn (ed. I. M. Arias, J. L. Boyer, W. Fausto, W. B. Jakoby, D. A. Schachter and D. A. Shafritz), pp. 447-473. Raven Press, New York.
- Rodriguez-Boulant, E. and Powell, S. K. (1992). Polarity of epithelial and neuronal cells. *Annu. Rev. Cell Biol.* **8**, 395-427.
- Samuelson, A. C., Stockert, R. J., Novikoff, A. B., Novikoff, P. M., Saez, J. C., Spray, D. C. and Wolkoff, A. W. (1988). Influence of cytosolic pH on receptor-mediated endocytosis of asialoorosomucoid. *Am. J. Physiol.* **254**, C829-C838.
- Sargiacomo, M., Lisanti, M., Groeve, L., Le Bivic, A. and Rodriguez-Boulant, E. (1989). Integral and peripheral protein compositions of the apical and basolateral membrane domains in MDCK cells. *J. Membr. Biol.* **107**, 277-286.
- Satir, P. (1994). Motor molecules of the cytoskeleton: Possible functions in the hepatocyte. In *The Liver - Biology and Pathobiology*, 3rd edn (ed. I. M.

- Arias, J. L. Boyer, N. Fausto, W. B. Jakoby, D. A. Schachter, and D. A. Shafritz), pp. 45-52. Raven Press, New York.
- Scheel, J. and Kreis, T. E.** (1991). Motor protein independent binding of endocytic carrier vesicles to microtubules *in vitro*. *J. Biol. Chem.* **266**, 18141-18148.
- Schiff, P. B. and Horwitz, S. B.** (1980). Taxol stabilizes microtubules in mouse fibroblast cells. *Proc. Nat. Acad. Sci. USA* **77**, 1561-1565.
- Simons, K. and Fuller, S. D.** (1985). Cell surface polarity in epithelia. *Annu. Rev. Cell Biol.* **1**, 243-288.
- Stockert, R. J., Morell, A. G. and Scheinberg, I. H.** (1976). The existence of a second route for the transfer of certain glycoproteins from the circulation into the liver. *Biochem. Biophys. Res. Commun.* **68**, 988-993.
- van Deurs, B., Peterson, O. W., Olsens, S. and Sandvig, K.** (1989). The ways of endocytosis. *Int. Rev. Cytol.* **117**, 131-177.
- Wandinger-Ness, A., Bennett, M. K., Anthony, C. and Simons, K.** (1990). Distinct transport vesicles mediate the delivery of plasma membrane proteins to the apical and basolateral domain of MDCK cells. *J. Membr. Biol.* **107**, 277-286.
- Watts, C. and Marsh, M.** (1992). Endocytosis: what goes in and how? *J. Cell Sci.* **103**, 1-8.
- Wheatley, D. N., Feilin, E. M., Yin, Z. and Wheatley, S. P.** (1994). Primary cilia in cultured mammalian cells: detection with an antibody against detyrosinated  $\alpha$ -tubulin (ID5) and by electron microscopy. *J. Submicrosc. Cytol. Pathol.* **26**, 91-102.
- Wolkoff, A. W., Klausner, R. D., Ashwell, G. and Harford, J.** (1984). Intracellular segregation of asialoglycoproteins and their receptor: A prelysosomal event subsequent to dissociation of the ligand-receptor complex. *J. Cell Biol.* **98**, 375-381.
- Wolkoff, A. W., Sosiak, A., Greenblatt, H. C., Van Renswoude, J. and Stockert, R. J.** (1985). Immunological studies of an organic anion-binding protein isolated from rat liver cell plasma membrane. *J. Clin. Invest.* **76**, 454-459.

(Received 8 August 1995 - Accepted 4 October 1995)